

NUMERICAL MODELLING OF WELDING OF CAR BODY SHEETS MADE OF SELECTED ALUMINIUM ALLOYS

In the paper, verification of welding process parameters of overlap joints of aluminium alloys EN AW-6082 and EN AW-7075, determined on the grounds of a numerical FEM model and a mathematical model, is presented. A model was prepared in order to determine the range of process parameters, for that the risk of hot crack occurrence during welding the material with limited weldability (EN AW-7075) would be minimum and the joints will meet the quality criteria. Results of metallographic and mechanical examinations of overlap welded joints are presented. Indicated are different destruction mechanisms of overlap and butt joints, as well as significant differences in their tensile strength: 110 to 135 MPa for overlap joints and 258 MPa on average for butt joints.

Keywords: EN AW-7075 alloy, CMT welding, hot cracks, mathematical model

1. Introduction

Nowadays, hybrid solutions are mostly applied in manufacture of car bodies, while, in some cases, only 2% to 10% of components are made of steel (in general, high-strength grades like Advanced High-Strength Steel [AHSS] or Press Hardenable Steel [PHS]) and the other components are made of sheet material of light alloys, mostly often aluminium alloys. Steel sheets are mostly used for components absorbing impact energy during a collision [1-3]. An example can be the door pillar B in the Audi A8, made of PHS steel [4].

Joining of car body components made of materials with diversified physico-chemical and mechanical properties, e.g. pillar B of PHS steel with the sill and roof profiles, encounters big difficulties of metallurgical nature [5]. Especially limited are traditional welding methods, i.e. fusion welding, where the joint is obtained as a result of melting and mixing together alloying components of the base material and the filler metal [5,6]. Mixing of alloying elements often initiates creation of hard and brittle intermetallic phases that adversely affect mechanical properties of the joints and, in the case of limited solubility of alloying elements, can also cause hot cracks in welds and/or in heat affected zone (HAZ) [6].

For this reason, traditional welding methods are replaced by friction stir welding (FSW), arc braze welding, most often with consumable electrode under active gas (MAG) or inert gas (MIG) shielding, and laser braze welding, more and more often multiple laser beam (Trifocal) welding [5-7].

Some car concerns are striving for complete elimination of steel at building car bodies from light alloys [4]. This enforces searching for new solutions that often come down to using high-strength aluminium alloys series 7xxx, like e.g. EN-AW 7075. They are multicomponent alloys with zinc, containing also magnesium and copper, commonly named zinc duralumins, showing best mechanical properties among all aluminium alloys [8]. They make a very favourable alternative for steel because, like high-strength steel, they make it possible to build a stiff passenger compartment playing the role of a safety cage [9]. However, the possibility to use car body elements made of aluminium alloys series 7xxx is conditioned by development of a suitable bonding technology that would guarantee obtaining high quality joints, highly aesthetic, with good mechanical properties. Unlike the commonly used alloys series 5xxx and 6xxx, the 7xxx alloys show low weldability resulting from relatively high copper content (over 1 wt%), which results in creation of intermetallic phases and can result in hot cracking in welds and/or in HAZ [10,11]. In addition, their welding by traditional methods results in dendritic structure in HAZ, leading to a drastic decrease of mechanical properties [11]. As is indicated in [12], use of laser welding or hybrid laser/GMAW for bonding EN-AW 7075 alloys increases the risk of hot cracking in the weld and in HAZ. Moreover, numerous gas pores are present in welds. The above imperfections are caused by too high power density of the integrated laser beam in comparison to arc welding methods, resulting in intensive evaporation of metal [12].

^{*} WROCLAW UNIVERSITY OF SCIENCE AND TECHNOLOGY, DEPARTMENT OF MATERIALS SCIENCE, STRENGTH AND WELDING, 5-7 LUKASIEWICZA STR., 50-370 WROCLAW, POLAND

^{**} WROCLAW UNIVERSITY OF SCIENCE AND TECHNOLOGY, DEPARTMENT OF METAL FORMING AND METROLOGY, 5-7 LUKASIEWICZA STR., 50-370 WROCLAW, POLAND

^{***} WROCLAW UNIVERSITY OF SCIENCE AND TECHNOLOGY, FACULTY OF MECHANICAL ENGINEERING, 5-7 LUKASIEWICZA STR., 50-370 WROCLAW, POLAND

[#] Corresponding Author: tomasz.wojdat@pwr.edu.pl

These days, bonding of the alloys series 7xxx is generally performed by mechanical method, of that clinching and self-piercing riveting (SPR) are most widespread [13-15]. In the case of welding methods, a solution can be application of modern power sources enabling strict control of heat amount introduced to the welding zone, using e.g. the reciprocating wire feeding (RWF) MIG technology. Nevertheless, obtaining joints with good mechanical properties will require very accurate selection of welding parameters within a very narrow range [7]. Moreover, quality and aesthetics of joints are favourably affected by robotization of welding processes, whose additional advantage is repeatability and higher capacity of the process. It is just high productivity, repeatability and possibility to obtain aesthetic joints with good mechanical parameters that are crucial aspects considered during developing a bonding technology for the automotive industry needs.

Therefore, the purpose of this research was determining the area of optimum parameters of welding aluminium alloys on the grounds of a digital FEM model and a mathematical model. It was also necessary to carry out empirical tests in order to verify the obtained results and to check, whether hot cracks are still present in the welds.

2. Materials and test methodology

Chemical composition of sheets of aluminium alloys EN AW-6082 and EN AW-7075 selected for the examinations is shown in TABLE 1 [17]. Thickness of the sheet metal was 3 mm. Over 1.20% of copper in the alloy EN AW-7075 favourably affects its mechanical properties, limiting however its weldability, especially with use of the methods where the base material and the filler metal are mixed together in the weld and the linear welding energy is high [10,16].

The joints to be examined were prepared by one of the most popular welding methods in the RWF MIG technology, i.e. the cold metal transfer (CMT) method. The choice was dictated by much smaller quantity of heat introduced to the welding zone in comparison to the traditional MIG method, which reduced the risk of hot cracking. This method is also profitable in economic terms, since it is highly suitable for application in robotized, flexible manufacturing lines.

The welding consumables in the CMT method are electrode wire and shielding gas. For welding of aluminium and its alloys, aluminium wires are used, most often containing additions of silicon (5 to 12 wt%) or magnesium (3 to 5 wt%) and smaller

amounts of other alloying elements like Ti or Zr, reducing resistance of the weld metal to hot cracking during solidification [17]. For welding of heat-treated aluminium alloys (EN AW-7075) that are more susceptible to hot cracking in welds because of their more complex metallurgical structure, usage of filler metals with different chemical composition is recommended, with lower (if possible) melting temperature and similar or lower mechanical properties [16]. Among others, filler metals based on the matrix Al-Si-Cu are recommended [16]. This is why the filler metal marked S Al 4047 (AlSi12) according to EN ISO 18273:2016-02 made by ESAB was chosen for the research. The selected filler metal contains an addition of titanium (ca. 0.15 wt%) that reduces the risk of hot cracking, and 12 wt% of silicon that, because of good deoxidizing properties, favourably reduces porosity of welds. As the shielding gas, argon 4.5 (99.99% Ar) was chosen.

Obtaining durable, functional joints with good mechanical properties required a technological analysis of the construction to be welded. According to the assumptions, elements of a passenger car body present in the joint connecting the pillar B with the sill and roof profiles were welded. The pillar B, made of EN AW-7075, is shaped by special cold working methods in such a way that it can be put on the sill and roof profiles made of EN AW-6082 to create an overlap joint. Therefore, trial joints were prepared in the analogous way, so that they reflected arrangement of the materials occurring in reality. However, it should be remembered that, in such a case, there is a problem to assess and control quality of the welded joints, since no suitable standards concerning such solutions exist. To that end, internal factory standards are used in the automotive industry, containing guidelines for the inspectors about acceptance of the executed welds. In most of European automobile companies (Volkswagen, Volvo etc.), for this type joints applied are the criteria containing minimum depth of fusion into the base material located at the bottom of the overlap joint. It is accepted that the joint meets the requirements, when fusion is at least 0.2 mm deep and is maintained on at least 1/3 of the weld width. In some cases, especially for less responsible joints transferring lower mechanical loads, minimum fusion depth of 0.1 mm is permitted.

In the considered case, arrangement of materials in the overlap joint, where EN AW-7075 is located on the top, is favourable. As a result, it is partially melted from the face only, which facilitates control of fusion depth, thus reducing the risk of hot crack occurrence. However, such an arrangement of materials need not occur in each constructional solution and it can happen

TABLE 1

Chemical composition of aluminium alloys according to EN 573-3:2014 [12]

Alloy	Chemical composition, wt%								
	Si	Fe	Cu	Mn	Mg	Cr	Zn	Ti	Al
EN AW-6082	0.70÷1.30	0.45÷0.55	0.08÷0.12	0.40÷1.00	0.60÷1.20	0.23÷0.27	0.18÷0.22	0.08÷0.12	Rem.
EDS analysis	0.99	0.47	0.09	0.50	1.13	0.26	0.19	0.08	Rem.
EN AW-7075	max. 0.40	max. 0.50	1.20÷2.00	max. 0.30	2.10÷2.90	0.18÷0.28	5.10÷6.10	max. 0.20	Rem.
EDS analysis	0.12	0.07	1.80	0.09	2.88	0.19	6.04	0.06	Rem.

that the materials are arranged in the reverse configuration. For this reason, joints prepared for two cases of mutual arrangements of base materials were also experimentally examined.

The risk of occurrence of hot cracks, especially during welding materials with limited weldability, can be minimised by welding with possibly lowest linear energy [18,19]. The amount of heat introduced to the weld depends on the welding linear energy. Its proper selection is significant, even when low-energy welding methods like CMT are applied. Linear energy of welding combines basic parameters of CMT welding, i.e. amperage, arc voltage and welding speed [16,18,19]. In order to determine the range of welding parameters, for which the risk of hot cracking would be minimum and the joints would fulfil the quality criteria, a mathematical model was developed. The input data were determined on the grounds of numerical simulation of the welding process. In the performed experiment, constant rate of the torch travel of 100 cm/min was applied. The variable quantity was amperage and the responding arc voltage was measured. Knowledge of these three parameters makes it possible to calculate linear energy in the welding process. The acquired data made it possible to adapt the numerical model and to verify it later.

3. Numerical and mathematical models

As was already mentioned, input data for developing the mathematical model were determined on the grounds of numerical FEM investigations. The discrete model of welding process of overlap joints of aluminium alloys was designed using the program Simufact Welding 6.0, dedicated for simulation of welding processes like pressure welding, soldering, arc welding, laser welding etc. Discrete models of overlap joints were created in the program Gmsh 3.0.6 and next exported to the environment Simufact Welding in order to model the heat source and course of the welding process. Dimensions of the modelled joints corresponded to real dimensions of the specimens cut-out of aluminium alloys EN AW-6082 and EN AW-7075 for experimental examinations. The specimens were shaped as rectangles 100×250 mm, arranged with an overlap 15 mm wide along the longer side.

On the grounds of the created numerical model, the area of permissible welding parameters with regard to depth and width of fusion was determined. It should be kept in mind that the FEM model is idealized, since the welding voltage can not be corrected within so wide range for each amperage value (i.e. to elongate and shorten the arc). The FEM model accepts such values, related to linear energy introduced to the weld. The welding parameters for that minimum fusion depth and width (Fig. 1a) were obtained according to the accepted evaluation criteria, determined on the grounds of the performed welding simulation, were: amperage 110 A, arc voltage 13.8 V and wire feed rate 5.5 m/min. In turn, extremely high values of welding parameters, determined also on the grounds of the performed numerical simulation (Fig. 1b) were: amperage 160 A, arc voltage 16.6 V and wire feed rate

7.0 m/min. The simulation was not continued for higher parameter values, since the risk of hot cracking in the weld or in HAZ significantly rises with increasing mixing degree of base metal and filler metal (larger fusion depth).

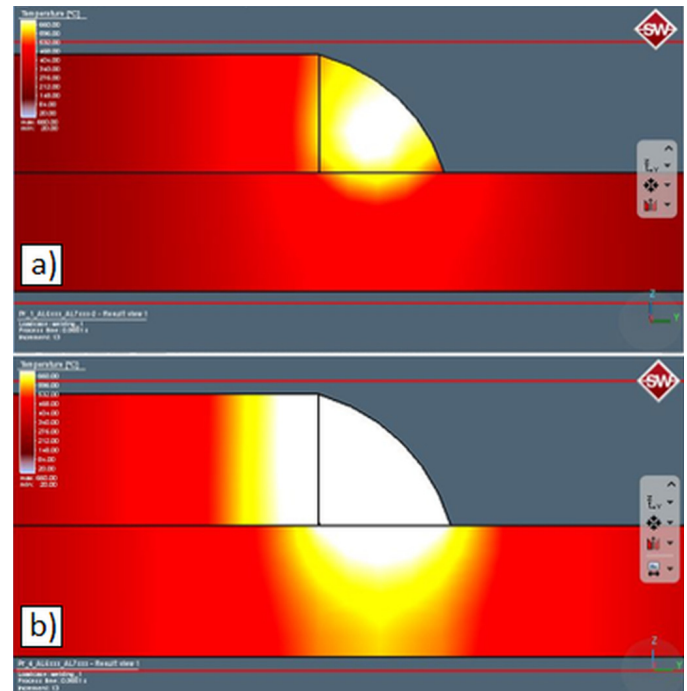


Fig. 1. Simulation results for welding parameters to obtain minimum required (a) and maximum fusion penetration (b)

The parameters determined on the grounds of the performed process simulation were used as input data for preparing the mathematical model. The function applied here was a third-degree polynomial for two variables (voltage and amperage), presenting the relationship between depth of fusion and width of the weld. For this purpose, the equations (1) and (2) were used [21]:

$$G_{w(I,U)} = p_{00} + p_{10} \cdot I + p_{01} \cdot U + p_{20} \cdot I^2 + p_{11} \cdot I \cdot U + p_{30} \cdot I^3 + p_{21} \cdot I^2 \cdot U \quad (1)$$

$$S_{w(I,U)} = p_{00} + p_{10} \cdot I + p_{01} \cdot U + p_{20} \cdot I^2 + p_{11} \cdot I \cdot U + p_{30} \cdot I^3 + p_{21} \cdot I^2 \cdot U \quad (2)$$

where: G_w – fusion depth [mm], S_w – weld width [mm], I – welding amperage [A], U – welding voltage [V].

The parameters determined from the numerical and the mathematical models were verified on the grounds of evaluation of the joints made for extreme and intermediate values of the welding parameters. Four overlap joints were prepared, in that the sheet EN AW-7075 was placed on the alloy EN AW-6082. Assessed was external appearance of the weld and its internal structure after cutting the joints in a transverse section. The joints were designated Z-1, Z-2, Z-3 and Z-4, subsequently from the smallest to the largest values of the welding parameters (Fig. 2).

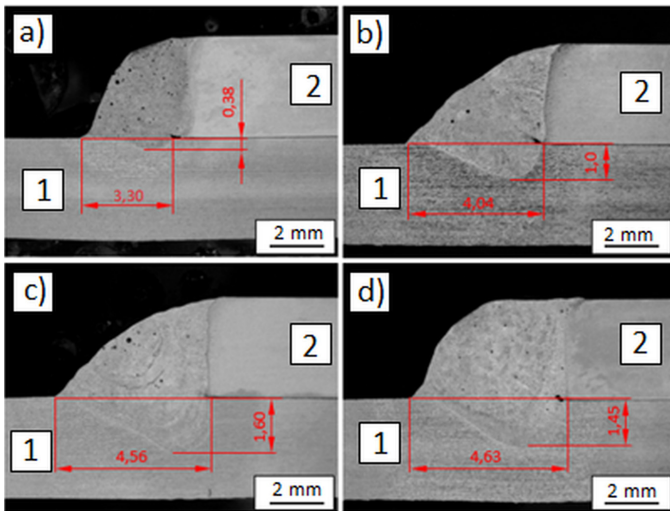


Fig. 2. Mathematical model showing permissible range of arc voltage and amperage to obtain the re-quired fusion depth and weld width

Summarizing, at the given arrangement of base materials in the joint, the optimum process parameters are those, for that the joints Z-3 and Z-4 were prepared. However, taking into account

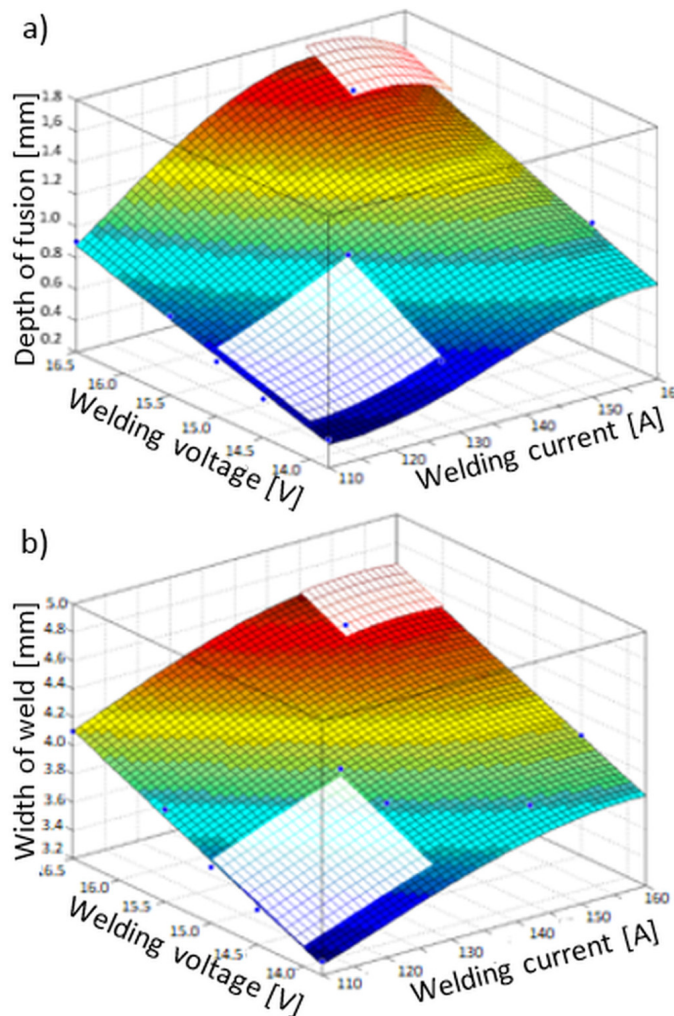


Fig. 3. Macrostructure of overlap welded joints of aluminium alloys: joint Z-1 (a), joint Z-2 (b), joint Z-3 (c) and joint Z-4 (d); alloy EN AW-6082 (1), alloy EN AW-7075 (2)

the reverse arrangement of the materials, where the alloy EN AW-6082 would be placed atop the EN-AW 7075, the parameters of the joint Z-1 seem more advantageous. This presumption is justified by the fact that the risk of hot cracks in EN AW-7075 decreases along with decreasing fusion depth (smaller mixing degree of metals). With reference to the above results, diagrams of the mathematical model were complemented with areas of optimum parameters depending on the way of arrangement of the base materials in the joint (Fig. 3).

4. Results and discussion

4.1. Microstructure of welded joints

Three welded joints were made and their parameters recorded during welding are shown in Table 2. Constant welding rate $V_s = 100$ cm/min was adjusted on the CMT heat source and values of the remaining parameters were resultant for the synergic line dedicated for welding materials up to 3 mm thick using electrode wire dia. 1.2 mm and controlled by wire feed rate (V_d). The following designations of individual joints were accepted: Z7-1 for the joint in that the alloy EN AW-7075 was placed on the EN AW-6082; Z6-1 and Z6-2 for the joints with reverse arrangement of base materials, made for extreme parameter values (maximum and minimum) from the determined range.

TABLE 2

Parameters of the welding CMT process of overlap joints

Joint number	Welding amperage, I [A]	Welding voltage, U [V]	Welding speed, V_s (mm/s)	Wire feed rate, V_d (m/min)	Welding energy, Q [kJ/mm]
Z7-1	160	15.9	16.6	7.12	0.12
Z6-1	111	14.1	16.6	5.64	0.08
Z6-2	162	16.2	16.6	7.05	0.13

Visual examinations with an unaided eye and with a magnifying glass ($6\times$) did not reveal any external cracks. Each weld was placed uniformly along the whole length of the joint, with no visible welding imperfections like open gas pores or spatters. The joints were characterised by high aesthetics, which is of particular importance at present tendencies observed in nearly all industries.

Microstructure of the weld is characteristic for the Al-Si system. It is composed of dendrites of α solid solution uniformly arranged in fine-grained eutectic mixture ($\alpha + \text{Si}$) (Fig. 4) [22]. The crystallisation direction of the weld coincides with the direction of heat abstraction from the joint, which is evidenced by characteristic arrangement of dendrites, solidifying from the base material towards the weld centre (Fig. 4a). The transition zone between the base material and the weld is significantly different for different alloys into that fusion occurs. The transition zone from the side of EN AW-6082 is much narrower, irrespective of its arrangement in the overlap joint (top or bottom). Within the fusion area, there are no visible changes in the base material structure (Fig. 4).

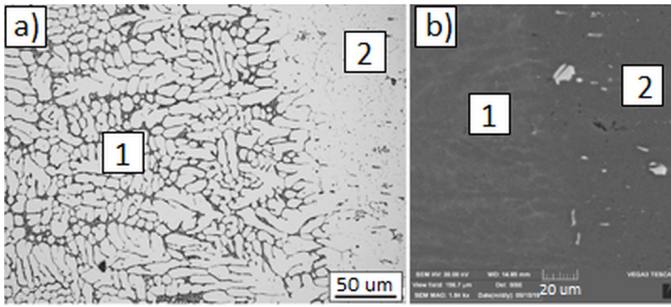


Fig. 4. Microstructure (a) and BSE image (b) of the joint in the transition zone from the side of EN AW-6082

From the side of EN AW-7075, the transition zone is clearly visible with its width much larger, ranging from 150 to 200 μm (Fig. 5). Visible is significant grain growth and dendritic structure, which can adversely affect mechanical properties of the alloy. In the joint Z7-1, in that EN AW-7075 was placed on the top of the overlap, as well as in the joint Z6-1 made in the reverse material arrangement and with lower welding parameters, no hot cracks are visible.

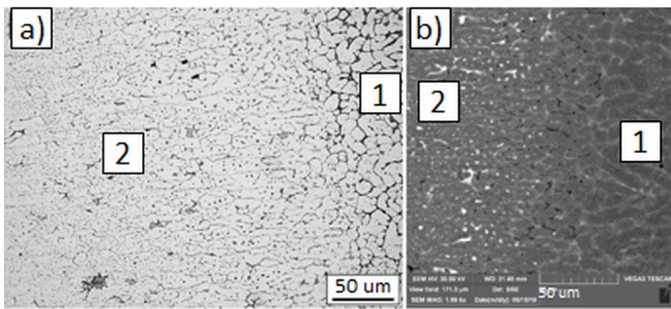


Fig. 5. Microstructure (a) and BSE image (b) of the joint in the transition zone from the side of EN AW-7075: 1 – weld, 2 – EN AW-7075

Increase of the welding parameters to the values for that the Z7-1 joint was prepared, but with reverse arrangement of the materials, resulted in occurrence of hot cracks in the weld and HAZ of the joint Z6-2 (Fig. 6). The mechanism that caused hot cracks in this zone is related to higher metal mixing degree in the weld, resulting from an increase of linear welding energy by nearly 0.05 kJ/mm. The cracks propagate on grain boundaries, along the bands created by cold working in the direction of

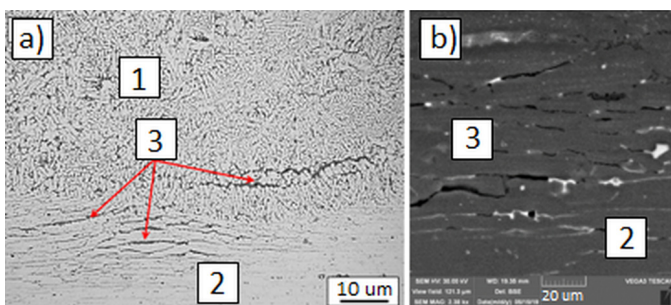


Fig. 6. Hot cracks (3) in the weld (1) and in the transition from the side of EN AW-7075 (2)

rolling the sheet material. As was indicated in [23,24], there is also high risk of hot cracking in HAZ during arc welding by the MIG-Puls method. Occurrence of the cracks is a consequence of improperly selected welding parameters, resulting in introducing too much heat to the joint (high linear energy).

4.2. Mechanical properties of welded joints

There are no relevant standards determining procedure of static shearing test of welded joints. Therefore, in industrial practice, the test can be carried-out using adapted guidelines of the standard EN ISO 4136:2013-05 concerning tensile test of butt welded joints. Test specimens are drawn and shaped like the butt-welded specimens. Static sharing test at tension was carried-out on a universal testing machine Zwick/Roell ZMARTPRO at the traverse speed of 0.2 cm/min.

Irrespective of the joint type, their mechanical strength was similar, ranging within 108 to 135 MPa (Fig. 7). Failure mechanism of the joints was also the same, with the fracture located in the weld, next to the base material placed on top of the overlap joint (Fig. 8). Five shearing tests were carried-out for each kind of the joint. In literature, no data concerning strength of overlap welded joints of aluminium alloy 7075 are reported. However, data concerning strength of joints spot-welded by FSW [24,26] or of MIG-welded cruciform joints [11] can be found. Strength of cruciform joints is on average 317 MPa and their fractures are located in both fillet welds. Therefore, strength calculated on one weld is ca. 158 MPa, except that there is no bending moment in this system.

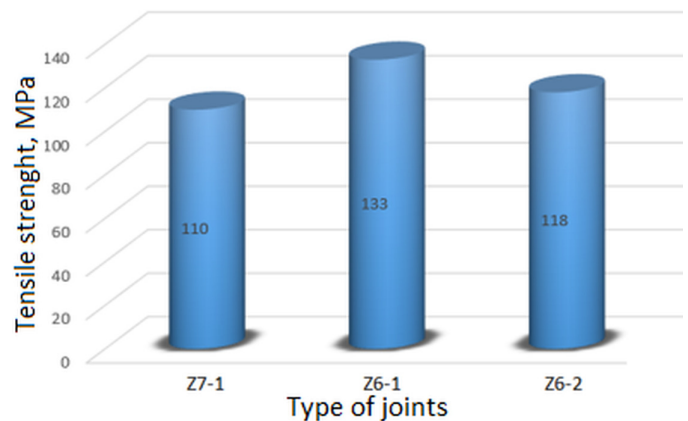


Fig. 7. Tensile strength of overlap joints

It should be emphasised that, during shearing of this type joints, a complex stress state is present, in that tensile stresses in the weld are accompanied by a bending moment. This moment certainly affects strength of overlap welded joints and the mechanism of their failure, which is proved by much higher strength of the joints made at similar parameters, but in the butt arrangement.

Strength of butt joints made for comparative reasons was over 2 times higher at 258 MPa on average and the fracture was

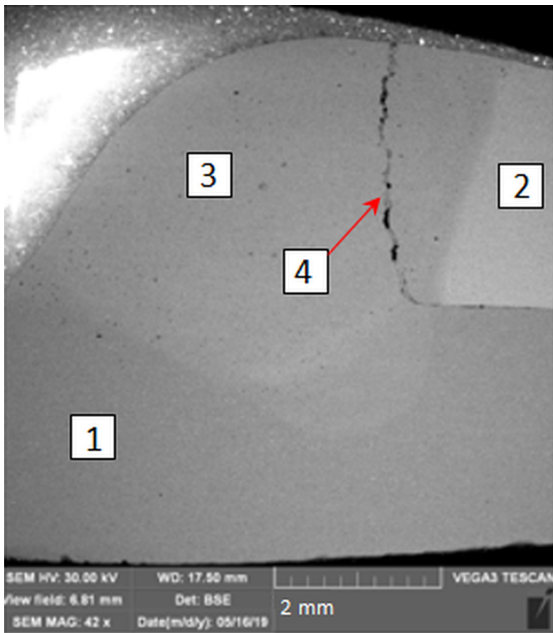


Fig. 8. Exemplary fracture of a Z7-1 type overlap joint after tensile test: 1 – EN AW-6082, 2 – EN AW-7075, 3 – weld, 4 – crack in the weld

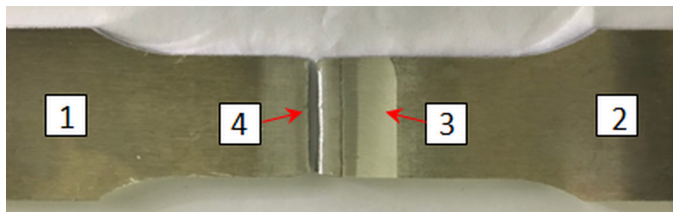


Fig. 9. Exemplary fracture in a butt joint after tensile test with a visible crack in the base material EN AW-6082

located outside the joint in the base material with lower tensile strength, i.e. in the alloy EN AW-6082 (Fig. 9). As reported in [16], tensile strength of similar butt joints of EN AW-7075 reaches even 587 MPa. In [27], results of tensile tests of dis-

similar butt joints of EN AW-7075 with EN AW-5083 made by FSW are presented, where the fractures were also located in the base material with lower strength (EN AW-5083) and tensile strength of the joints was on average 370 MPa.

Vickers hardness measurements were made according to EN ISO 6507-1:2007 [28], at the selected load of 50 G for small joints, suitable for a narrow HAZ. The measurement covered all zones of the weld: the base material (BM), the heat-affected zone (HAZ) and the weld (W). Distances of $3d$ (d = indentation diameter) between individual indentations complied with the standard guidelines. Arrangement of materials in the overlap joint did not significantly affect hardness distribution. The highest hardness of ca. 143 HV0.05 on average occurred in the base material EN AW-7075 and the lowest hardness of ca. 82 HV0.05 occurred in the other base material EN AW-6082. Hardness in the weld was uniform between 92 and 99 HV0.05. In the alloy EN AW-7075, structural changes were revealed in HAZ, where dendritic structure was created and grain growth occurred, accompanied by lower hardness. Hardness decreased from ca. 140 HV0.05 in the transition zone at the boundary with the base material down to 100 HV0.05 in the transition zone at the boundary with the weld. A similar relationship was revealed in [27] in the joints welded by FSW, where aluminium alloys EN AW-5083 and EN AW-7075 were bonded. Hardness distributions in individual joints were similar, so the distribution in the joint Z7-1 only is shown (Fig. 10).

5. Conclusions

The carried-out experimental examinations prove rightness and high effectiveness of numerical and mathematical modelling of welding processes. The models are effective tools making it possible to determine ranges of permissible process parameters with no necessity to carry out experimental examinations, often very much time- and cost-consuming. This of high importance

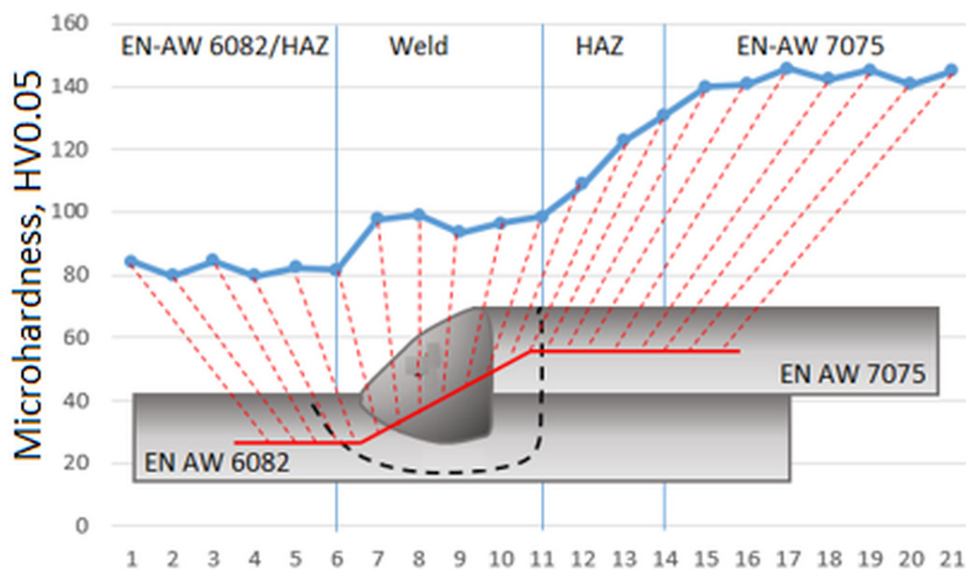


Fig. 10. Hardness distribution in the overlap joint Z7-1

at prototyping and designing new welding technologies, especially for the materials with limited weldability or heterogeneous materials.

Moreover, the following conclusions can be drawn from the obtained results:

- It is possible to obtain functional joints of the aluminium alloy EN AW-7075 with no hot cracks. However, this requires strict controlling the amount of heat introduced to the weld, which is possible with use of new low-energy welding technologies GMAW.
- Strength of overlap welded joints does not depend on mutual arrangement of base materials and is on average 120 MPa. This is strongly affected by complex state of stress in the joint, in that a bending moment acts apart from tensile stresses.
- In the case of butt joints, failure occurs in the base material of lower strength, i.e. in the aluminium alloy EN AW-6082.
- In spite of low welding energy in the CMT technology, a HAZ up to 200 μm wide occurs in the alloy EN AW-7075, where the dendritic structure is visible.
- Even a small increase of the welding linear energy (by ca. 0.05 kJ/mm) affects the possibility of hot cracking in the alloy EN AW-7075, resulting in deeper fusion and thus higher mixing degree with the filler metal.
- Hardness of the alloy EN AW-7075 in HAZ is reduced even by over 30 HV0.05.

REFERENCES

- [1] W.S. Miller, L. Zhuang, J. Bottema, A.J. Wittebrood, P. De Smet, A. Haszler, A. Vieregge, Recent development in aluminium alloys for the automotive industry, *Materials Science and Engineering* **280**, 37-49 (2000).
- [2] J. Hirsch, Recent development in aluminium for automotive applications, *Transactions of Nonferrous Metals Society of China* **24**, 1995-2002 (2014).
- [3] J. Hirsch, Automotive trends in aluminium – The European perspective, *Materials Forum*, 15-23 (2004).
- [4] The aluminium automotive manual, Applications – Car body – Body structure, 2-83 (2013), online pdf.
- [5] Z. Mirski, T. Wojdat, A. Margielewska, Braze-welding in joining dissimilar materials, *Biuletyn Instytutu Spawalnictwa w Gliwicach* **3** (62), 26-32 (2018).
- [6] W. Gawrysiuk, Technology of braze welding by arc methods. Technological recommendations and examples of application in industry, *Biuletyn Instytutu Spawalnictwa* **3** (49), 35-40 (2005).
- [7] T. Pfeifer, S. Stano, Modern methods of weldbrazing in the aspect of quality and properties of joints, *Welding Technology Review* **9** (88), 95-102 (2016).
- [8] EN 573-3:2014 Aluminium and aluminium alloys – chemical composition and form of wrought products – Part 3: chemical composition and form of products.
- [9] The aluminium automotive manual, Joining – Introduction, 1-5 (2015).
- [10] Ł. Bolewski, M. Szkodo, P. Pękala, Investigation of the impact in current intensity on AW-7075 aluminum alloy welding, *Projektowanie i Konstrukcje Inżynierskie* (9), 22-26 (2016).
- [11] Ł. Bolewski, M. Szkodo, P. Pękala, G. Ochocki, Impact of shielding gases composition on AW-7075 aluminum alloy welding, *Projektowanie i Konstrukcje Inżynierskie* (3), 20-24 (2017).
- [12] M. Kang, Ch. Kim, A Review of Joining Processes for High Strength 7xxx Series Aluminum Alloys, *Journal of Welding and Joining* **6** (35), 79-88 (2017).
- [13] G. Meschut, V. Janzen, T. Olfemann, Innovative and Highly Productive Joining Technologies for Multi-Material Lightweight Car Body Structures, *Journal of Materials Engineering and Performance* **5** (23), 1515-1523 (2014).
- [14] O. Hahn, G. Meschut, S. Suellentrop, V. Janzen, T. Olfemann, *Joining Technologies in Hybrid Lightweight Structures*, *Leichtbau der Fahrzeugtechnik*, Springer Vieweg Verlag, Wiesbaden, Germany, 622-662 (2013).
- [15] The aluminium automotive manual, Joining – Mechanical joining, 1-66 (2015).
- [16] J. Pilarczyk (red.): *Engineer's guide. Welding*, Vol. 1, WNT Publishing (2003).
- [17] DIN EN 485-2:2018 Aluminium and aluminium alloys – Sheet, strip and plate – Part 2: Mechanical properties.
- [18] E. Tasak, A. Ziewiec, *Weldability of construction materials*, Vol. I, *Weldability of steel*, JAK Publishing, (2009).
- [19] E. Tasak, A. Ziewiec, Characteristics of cracks in welded joints and methods of prevention, *Bonding of Metals and Plastics in Practice* (2), 10-15 (2017).
- [20] EN ISO 14175:2009 Welding consumables – Gases and gas mixtures for welding and related processes.
- [21] <https://www.mathworks.com/help/curvefit/fit.html>
- [22] T.B. Massalski, *Binary alloys phase diagrams*. Vol. 1, ASM International, (1992).
- [23] T. Pfeifer, J. Rykała, Welding EN AW 7075 Aluminium Alloy Sheets – Low-energy Versus Pulsed Current, *Biuletyn Instytutu Spawalnictwa* **5** (58), 137-144 (2014).
- [24] I. Peter, M. Rosso, Study of 7075 aluminium alloy joints, *The Scientific Bulletin of VALAHIA, University MATERIALS and MECHANICS* **13** (15), 7-11.
- [25] EN ISO 4136:2013-05 Destructive tests of welded metal joints - Tensile test of transverse specimens.
- [26] Z. Liu, K. Yang, D. Yan, Refill Friction Stir Spot Welding of Dissimilar 6061/7075 Aluminum Alloy, *High Temperature Materials and Processes* **39**, 69-75 (2019).
- [27] I. Kalemba, D. Miara, M. Kopyściański, K. Krasnowski, Characterization of friction stir welded 5xxx and 7xxx aluminum alloys, *Welding Technology Review* **2** (87), 30-36 (2015).
- [28] EN ISO 6507-1:2007 Metals – Vickers hardness measurement – Part 1: Test method.